Research & Reviews: Journal of Material Sciences e-ISSN: 2321-6212

Flexible, Polymer-Based Microwave Devices: Flexible Antennas and Performance Evaluation

Iurii Cherukhin[1]*, Siping Gao[1], Felix Zander[2], Alena Dashkova[3], Yong Xin Guo[1]

[1]Department of Electrical and Computer Engineering, National University of Singapore, 4 Engineering Drive 3, 117583, Singapore

[2]Department of Radioelectronic Systems, Siberian Federal University, Kirenskogo Street, 28, 660074, Krasnoyarsk, Russia

[3]Department of Radioelectronic Systems, Siberian Federal University, Kirenskogo Street, 28, 660074, Krasnoyarsk, Russia

Research Article

Received: 28-Mar-2024, Manuscript No. JOMS-24-130904; **Editor assigned:** 01- Apr-2024, PreQC No. JOMS-24-130904 (PQ); **Reviewed:** 15- Apr-2024, QC No. JOMS-24-130904; **Revised:** 22- Apr-2024, Manuscript No. JOMS-24-130904 (R); **Published:** 29-Apr-2024, DOI: 10.4172/2321-6212.12.1.005

***For Correspondence:**
Iurii Cherukhin, Department of Electrical and Computer Engineering, National University of Singapore, 4 Engineering Drive 3, 117583, Singapore

E-mail: FZander@sfu-kras.ru

Citation: Cherukhin L, et al. Flexible, Polymer-Based Microwave Devices: Flexible Antennas and Performance Evaluation. RRJ Mater Sci. 2024;12:005.

ABSTRACT

In this work, we have investigated polymer-based flexible antennas from commercial and modified polymers, which are competitive to rigid PCB technology. Classical designs of the patch and bow-tie antennas have been realized and showed that the realized gain can get up to 9.16 dBi for the patch and 7.9 dBi for the bow-tie antennas. The effects of the dielectric loss and conductivity on the antennas' performance in S-band have been analyzed in order to find limits for further material engineering and the optimum trade-off between microwave and mechanical performance. The bending effects have been investigated, and it has been found that e-plane bend inside can have the focusing effect and boost the antenna gain from 8.6 dBi to 10.1 dBi with the frequency shit from 2.5 GHz to 2.4 GHz for the patch and 7.9 dBi to 11.3 dBi at 3.1 GHz for the bow-tie antennas. The non-classical π-shaped conductors' edges lead to additional fringing fields, which has an effect on the antenna's gain, which can be exploited for further performance improvements. The new recipes for low-loss, low-Dk dielectric materials, and chemical integration between conducting polymers and PDMS have been presented in this work. The current molding process allows us to step out from 2D PCB designs and build 3D structures or hybrid PCB-3D components with a certain freedom in material properties. Additionally, the new material exhibits unique mechanical properties, i.e., low density, temperature insulation, vibration and acoustic dumping effects, low humidity absorption, etc., which extends the material application to other fields.

Keywords: PDMS; Flexible antenna; Fillform; Patch antenna; Bow-tie antenna; Conductive polymer

INTRODUCTION

Flexible microwave electronics is an emerging technology and has all chances to stand along with the common commercial technology such as PCB and metal waveguides. The applications of flexible electronics are not limited by wearable devices. Mechanical flexibility allows withstanding significant distortions without the destruction of the devices. This feature can be exploited under extreme operational conditions like rapid acceleration, immense vibrations, various deformations, including twisting, bending, and stretching.

The flexible microwave electrons can be roughly divided into few groups by types of conducting and dielectric materials, i.e., semi-ridged which are based on very thin Roger, Duroid, or LCP substrates with copper cladding; thin-flexible which are based on PEN (Polyethylene Naphthalate), PET (Polyethylene Terephthalate) and Kapton (polyimide) and similar rigid polymers with copper cladding or 3D printed Ag-inks; polymer-based which are produced fully or partially from elastomers and can have substrate thickness more than 1 mm without significant impacts on the flexibility [1-8].

Fully polymer-based microwave devices can be produced in hybrid-PCB or fairly complex 3D structures with variations in mechanical and electrical properties. Such an approach provides additional freedom for designs, greatly extends the possible areas of applications and working conditions.

The requirements for the microwave devices are quire strict, i.e., surface roughness, dimension tolerances, electrical properties of materials, additional requirements for flexibility, and many others. We will demonstrate in this work that some requirements could be mitigated or varied in order to achieve the optimum balance between microwave performance and mechanical flexibility by implementing suitable production technology and material engineering. The first approach to answer this question has been demonstrated in our previous works [9,10].

MATERIALS AND METHODS

The classical designs of a patch antenna and slotted bow-tie antennas have been chosen to evaluate the effect of materials properties, i.e., the dielectric loss and conductivity on antennas performance under flat and bent conditions. The classical design allows looking at the antennas' performance regardless of improvements in designs (improved gain, bandwidth), which, of course, can be implemented on the sequential development steps of flexible polymer-based electronics.

The slotted bow-tie antenna is a wideband antenna and does not require any baluns in the feeding network and requires only one layer of "metallization". The patch antenna is resonance-type antenna, where the dielectric loss might have a dominant effect on the performance rather than conductivity. The patch antennas require two layers of "metallization". The different layer configuration has a direct influence on the bending performance. The strain-stress deformation pattern is different in both cases and has different effects on the antenna's mechanical and microwave performance.

Material discussion dielectric elastomers

The various elastomers have been analyzed, including several grades of PDMS (polydimethylsiloxane), i.e., Sylgard 184, Sylgard 170, MS1002, SE 1740, EG3896, SE 7450 from dow Chemical, natural latex, elastomers for 3D printing, co- polymers, and many others. The results of the analysis with selection criteria have been described [11]. Based on the criteria for flexible microwave electronics, a new compound has been developed, which consists EG-3896 PDMS gel, DET or 3M microspheres, and other components.

The combination of EG-3896 and microspheres has a unique microwave and mechanical properties, e.g., excellent stretch ability, low dielectric loss, low dielectric constant, moisture absorption less than 0.067%, vibration dumping capabilities, etc. Figure 1 shows the comparison Sylgard 170 with the compound of EG-3896 with vol. 50% K20 microspheres as modified PDMS. The dielectric loss became 0.0034 at 2.6GHz, and it is already comparable to commercial, rigid PCB substrates like RO4003C or RO4350B, which have dielectric loss 0.0027 and 0.0037 accordingly.

Figure 1. Measured dielectric constants and tan loss of modified PDMS and Sylgard 170. The waveguide transmission line method was used for these measurements.

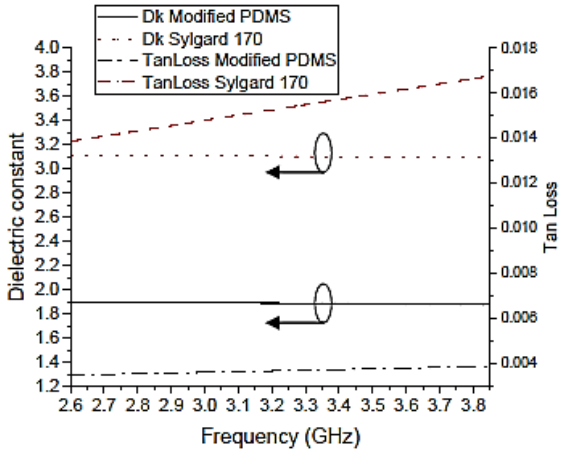

The further improvements have been archived with a recipe EG3896+vol. 50% DET 40+3% 7558 co-polymer. Such combination gives no variations of dielectric constant over frequency in the wideband from 2.6 GHz–12.5 GHz and very small dielectric loss, i.e., Dk is equal to 1.73 and dielectric loss is 0.001 ± 0.0005 at 2.6 GHz to 3.95 GHz and 0.01-0.014 at 8.4 GHz to 12.5 GHz, even though the material samples have been cured at 100C.

Conducting polymers

Another critical component in polymer-based microwave electronics is a conducting polymer with the ability to stretch from 1% to 3%. The conducting polymers from EMS (CI series), DuPont (PE873), and Dow Chemical (DA6534) companies were purchased and tasted (Table 1). The “uncured” state of such polymers consists 60% silver nanoparticle in either polymer matrix with solvents in the case CI series or PDMS based matrix in cased DA6534. The measurements have been done by the 4-point probe technique. Our purchased CI series conducting polymers are having slightly different conductivity, viscosity, surface roughness, stretching, and bending abilities than it has been stated in the data-sheets except for DA6534 from Dow.

Table 1. Summarizes the data from the data-sheet and measured conductivity.

Name	Data-sheet conductivity (S/M)	Measured conductivity (S/M)
CI-1036	$3.9*10^6$	$1.6*10^6$
CI-1036 mod	_	$6.75*10^6$

CI-1075	$3.6*10^6$	$4.2*10^6$
CI-4040	$0.78*10^6$	$0.7*10^6$
DA6534	$0.55*10^6$	$0.45*10^6$

The conducting polymers can be modified to tune the required properties. The conductivity can be increased by rising metal filling proportion either in the bulk material or at the interface between the substrate and conducting layer by additional passivation with metal particles [12]. By trying various methods, we have found experimentally that the most straightforward approach (in terms of implementation and integration in our production process) is to add a very small amount of conducting particles with a very large aspect ratio (length to diameter ratio) [13]. Copper nanotubes and copper nanowires would be the best solution in such a case, but it is still not available commercially. We used copper bonding wires with 50 um in diameter and chopped at length from 10 to 30 mm. The length has been chosen arbitrary based on the required device's dimensions and stretchability. Such short wires could be evenly distributed either in the volume of "uncured" polymers or on the surface. The conductivity of CI-1036 has been increased 4 times by implementing this way.

The mechanical and temperature deepened properties of CI series are discussed [11]. Although, it worth mentioning that Dow DA6534 is PDMS-based with good mechanical properties, and the chemical adhesion happens naturally with PDMS dielectric substrates.

Production

Based on molding technology, we have developed our production process, which allows flexibility in terms of used polymers and curing conditions. The detailed description of the production process and chemical integration among different polymers have been described [11]. Figure 2 Illustrates the mold for the bow-tie antenna. All parts are made from PTFE (Figure 3).

Figure 2. The mold for the bow-tie antenna and CPW line**.**

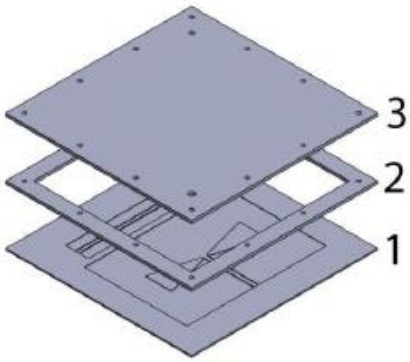

Figure 3. The cross-section of the edge of produced microstrip line from Sylgard 170 and PE873.

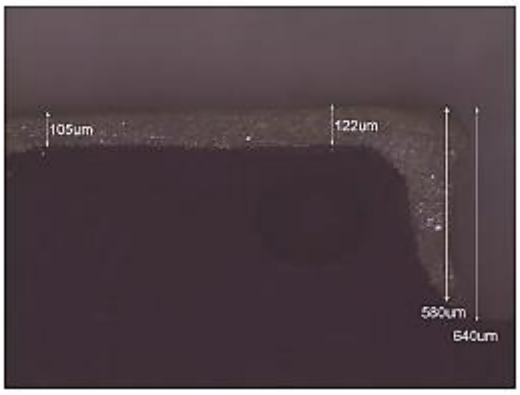

The current production process has several aftermaths on the final products. One of them is a distinctive cross-section of produced conducting layers. It has π shapes and is illustrated in Figure 4. This shape increases coupling effects to the nearest lines. By varying the initial volumes and shapes for conducting and dielectric layers, we can produce not only planar structures but complex, full 3D geometries. This opens another degree of freedom for engineering filters, antennas, and many other microwave devices. Following the described production technology, we have produced several sets of CPW fed bow-tie antennas and microstrip fed patch antennas (Table 2).

Figure 4. Produced a) patch antenna and micro strip line, b) slotted bow-tie antenna, and CPW line.

a)

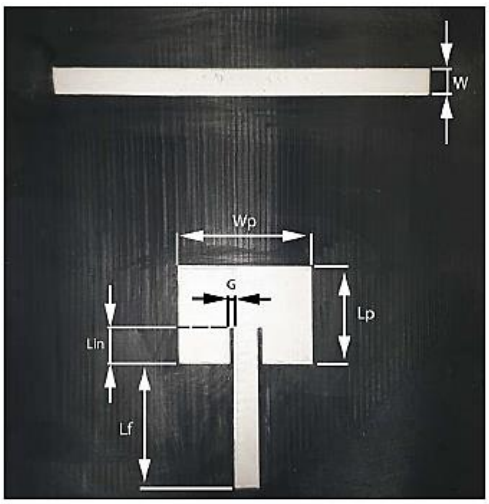

b)

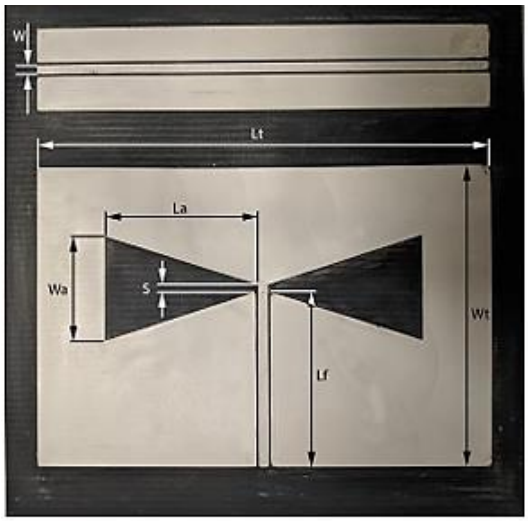

Table 2. shows variations of used materials in our investigation.

Produced antennas				
	Bow-tie antenna		Patch antenna	
	Sylgard 170	EG3896-microspheres	Sylgard 170	EG3896-microspheres
CI-1036	+	-	+	-
CI-1036 mod	+	+	+	+
CI-1075	+	-	+	-
CI-4040	+	+	+	+

DA6534	+	-	-	+
Note: (+) Used Materials,(-) Unused Materials.				

Combinations of Sylgard 170 with different conducting layers should show the effect of conductivity on the device's performance in flat and bent conditions, while combinations EG3896 with 50% microspheres (further on as gel or modified gel) with the worse and the best conductivity should show the effect of the dielectric loss on the performance. DA6534 is used with two different dielectrics for illustrative purposes due to the limited amount of the material. PE873 is excluded from the further discussion due to DuPont's restrictions (Table 3).

Table 3. shows the dimensions of designed and produced antennas.

Antennas dimensions (MM)		
Sylgard 170 (ε=3.1)		Modified gel (ε=1.85)
Patch antenna		
W	8.1	11.5
G	1.3	2.4
Lp	32.26	41.2
Wp	44.65	51.5
Lin	11.5	12.8
Lf	40	40
Bow-tie antenna		
W	2.4	3.9
CPW gap	0.4	0.5
La	45.2	52.64
Wa	27.5	27.2
S	1.1	0.5
Lf	49.45	54.75
Wt	85	110
Lt	130	150

The substrate thickness is 3 mm in all cases, which illustrates the fair approach for being flexible. Many materials that are used in the "flexible" electronics can be considered flexible only with extremely small thicknesses (100 um or less), e.g., polyimide (Kapton), polyethylene, PTFE, and others. CPW gaps for Dk 3.1 and 1.85 are very close due to an additional increase in the coupling by the rising height of the π-shaped "metallization" in the cross-section. The "metallization" thickness exceeds 5 skin depths in all cases. DA6534 has 350 um in thickness since it does not have any shrinkage.

Connectors

The conducting polymers CI series and PE873 allows to solder connectors with low-temperature eutectic alloys. However, the point contact enforces additional stress in a very small area, which leads to cracks and tears. To resolve these issues, the SMA Radiall (R125.541.000) end-launch connectors were modified in such a way that it allows connections without soldering. Figure 5 illustrates configurations for CPW and microstrip connection. The dark grey parts have been printed on a 3D printer from aluminum alloy.

Figure 5. Custom made SMA connectors for a) microstrip and b) for CPW application.

This configuration allows using connectors with very thick substrates up to 8 mm, adjustable CPW pitch, fast connection and reconnection, and repeatable connection from one set-up to another. The conducting silver paint has been used at the edges to ensure proper ohmic connection and to mitigate excessive loss due to oxidation layers.

RESULTS AND DISCUSSION

Measurements

S-parameters measurements have been done on PNA N5227A with custom SMA end-launch connectors (Figure 6). Special support has been designed and produced to provide rigid support for antennas in flat and bent conditions, and at the same time, it does not disturb the antenna's performance. Bending conditions have been carried out by applying antennas on the polyfoam cylinders with various diameters (200, 150, 100, and 75 mm).

Figure 6. Illustration of bending conditions for patch and bow-tie antennas a) E-plane bend inside, b) H-pane bend inside, c) E-plane bend outside, d) H-plane bend outside.

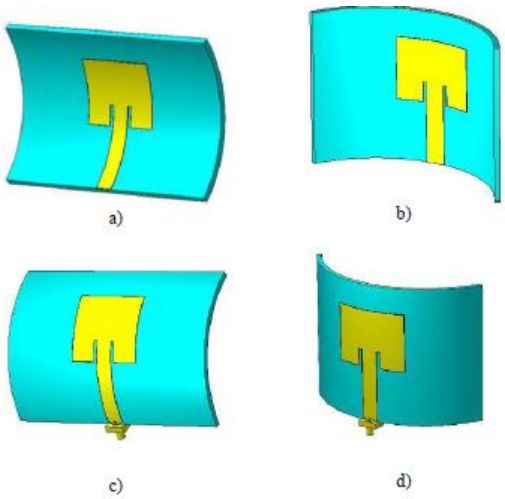

The radiation patterns have been measured in an anechoic chamber. It is necessary to mention that our anechoic chamber does not have an automatic system for seeking maximums in the boresight. All adjustments have been done manually, and it is possible that some of the measurements are slightly off. The radiation patterns have been measured in horizontal and vertical scanning, including cross-polarizations. Only selected data is shown in the publication due to the page limitation.

S-parameters of flat antennas

The reflection coefficient measurements of the patch and bow-tie antennas without any deformation are shown in Figures 7-10 and compared with simulated results in CST studio. The dimensions of produced antennas have 30 um or less difference with simulated parameters in xy-plane and 100 um in z-plane. However, π-shaped edges should contribute to the fringing fields to the ground and to the nearest metallization's, like the in the insert gaps of

the feeding networks. The frequency shifts about 30 MHz and less might be associated with the additional fringing fields. It has been noticed that less accurate meshing in CST studio produces lesser frequency difference with measured data. Ripples in Figures 9 and 10 are due to the excessive amount of points in the measured data, plus the final feeding network impedance is slightly different from 50 ohms. Additionally, the insertion loss is 0.1- 0.2 dB higher in the measured data due to custom-made connectors and trimmings.

Almost all reflection coefficients illustrate that less conductive polymers produce better matching, except DA6534. This is explained by additional ohmic losses in the conductors, which reduces reflection power from the antennas. As mentioned before, DA6534 has no shrinkage, and produced patch antennas and micro strips have 300 um less gap between the ground and signal planes, which indeed increases reflection due to impedance mismatch.

The expected effect of conductivity on the resonance type of antennas is in the bandwidth. Fewer losses must sharpen S11 and produce a narrow bandwidth. Figure 7 illustrates perfectly how CI-4040 gives 90 MHz bandwidth, and then it gradually narrows down to 80 MHz with modified CI-1036. However, the exact opposite effect with the low-loss dielectric in Figure 8. Modified CI-1036 gives 124MHz bandwidth, CI-4040–103 MHz, and DA6534–97 MHz.

Figure 7. Measured and simulated S11 parameters for the patch antenna with Sylgard 170 as dielectric and various conducting polymers.

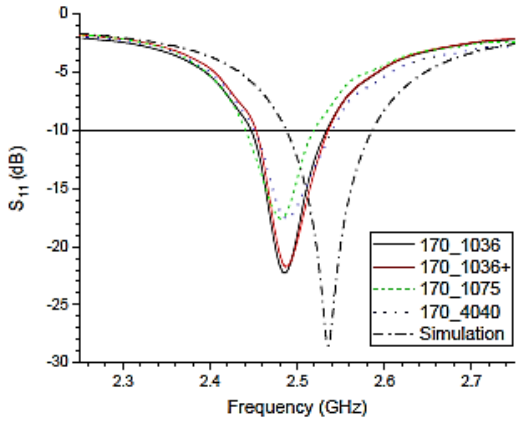

Figure 8. Measured and simulated S11 parameters for the patch antenna with modified EG3896 as dielectric and various conducting polymers.

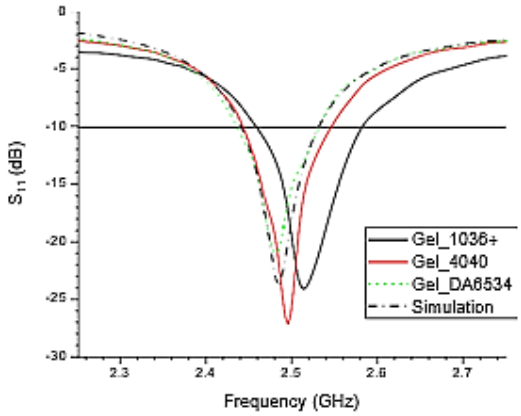

A similar picture has been observed for the bow-tie antennas. Sylgard 170 with modified CI-1026 has 815 MHz bandwidth, CI-1075–975 MHz, CI-4040–1006 MHZ, but again the exact opposite effect in with low loss dielectric in Figure 10, i.e., modified CI-1036–790 MHz and CI-4040 645 MHz.

The bow-tie with combination CI-4040 and patch antenna with CI-1036+ and modified EG3896 have been chosen to illustrate the effect of bending on the reflection coefficient and radiation patterns. Both antennas have been deformed. Only selected graphs are shown for the illustration of expected and unexpected cases.

Figure 9. Measured and simulated S11 parameters for the bow-tie antenna with Sylgard 170 as dielectric and various conducting polymers.

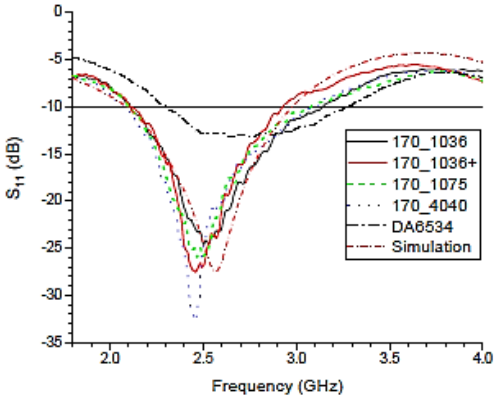

Figure 10. Measured and simulated S11 parameters for the bow-tie antenna with modified EG3896 as dielectric and various conducting polymers.

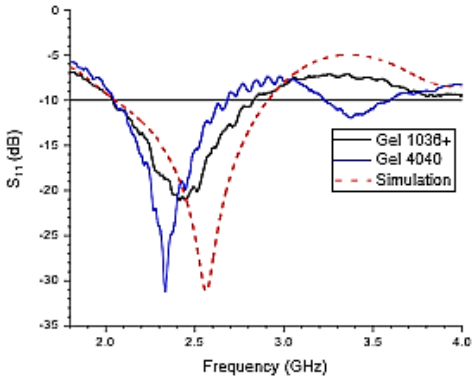

S-parameters of bent antennas

Any bending conditions induce tension and compression forces on the surface and in the bulk of the materials. These forces will deform the material with respect to the elastic properties (Young's modulus) of such materials. The Young's modulus of PDMS is in the range 300-600 KPa; CI conducting polymers is in MPa range, while the most used Kapton and Copper are in GPa range and can be flexible within very specific conditions.

Figure 11 shows the expected frequency shift and variations in the reflection coefficient of the patch antenna. The most deformation is in the substrate thinning due to unequal Young's modulus of materials and just a small portion in the compression and stretching of the physical dimensions of the conducting layers. E-plane bend inside gives the increase in the bandwidth by 10 MHz at the curvature diameter 75 mm in the measured and 20 MHz in the simulated results compare to the flat condition. H-plane bend inside gives the bandwidth reduction to 97 MHz at D200, 93 MHz at D150, and 51 MHz at D75 in the measured data and 73 MHz at D200, 68 MHz at D150, 34 MHz at D75 in the simulated data.

Figure 11. Measured and simulated S11 parameters for the bent in E-plane inside patch antenna with modified EG3896 as the dielectric.

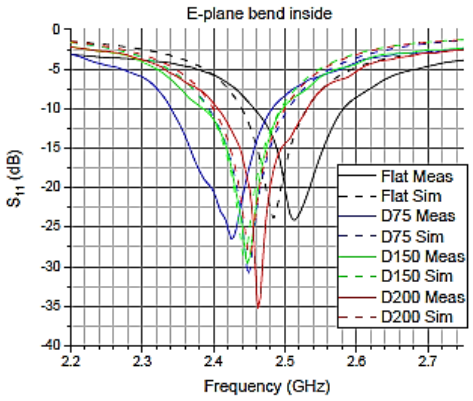

E-plane bend outside shows in Figure 12 the abnormal frequency shift. The simulation results indicate that the lower the curvature diameter–the lower the operating frequency would be. Such results are well understood if the signal plane would stretch enough. However, the stiffer conducting plane enforces rather a compression of the substrate than stretching. CST simulations with correct values of Young's modulus and Poisson's coefficients cannot accurately predict physical deformations. It is possible that Ansys could make a better prediction. Nevertheless, both types of deformations result in the impedance mismatch versus curvature diameter. E-plane bend outside gives 25 MHz reduction in the bandwidth at the curvature diameter 75 mm in the measured and 34 MHz in the simulated results compare to the flat condition. H-plane bends outside gives an increase in the bandwidth to 143 MHz at D200, 130 MHz at D150, and 160 MHz at D75 in the measured data and 97 MHz at D200, 98 MHz at D150, 99 MHz at D75 in the simulated data.

Figure 12. Measured and simulated S11 parameters for the bent in E-plane outside patch antenna with modified EG3896 as the dielectric.

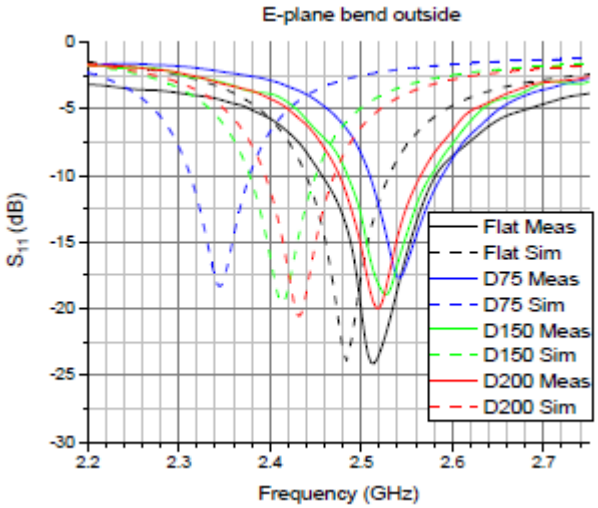

The bow-tie antenna has only one layer of dielectric and conductor, and bending inside or outside will have similar results in the impedance mismatch. The bi-directional, symmetrical radiation pattern can provide information about both types of bending with one measurement. Figure 13 illustrates the similar effects with the patch antenna. The impedance match is getting worse with the reduction of curvature diameter in measured data. The operational frequency shifts left with a simultaneous reduction in the bandwidth by 87 MHz with D100 compare to the flat

condition in measured and simulated data. Although, the E-plane bend outside simulation data shows a slight increase in the operational frequency.

Figure 13. Measured and simulated S11 parameters for the bent in E-plane outside bow-tie antenna with modified EG3896 as the dielectric.

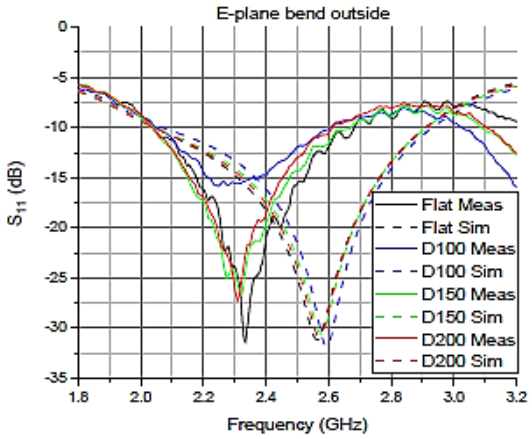

The H-plane bend outside (Figure 14) indicates some improvements in the impedance match. The bandwidth slightly improves from 645 MHz in the flat condition to 706 MHz at D200 and then reduces to 560 MHz at D150 and 459 MHz at D100 in the measured data. Simulation results show 947 MHz bandwidth in the flat condition, 844 MHz at D200, 836 MHz at D150, 790 MHz at D100. The maximum bandwidth shift is 186 MHz and 157 MHz in the measured and simulated data, respectively.

Figure 14. Measured and simulated S11 parameters for the bent in H-plane outside bow-tie antenna with modified EG3896 as the dielectric.

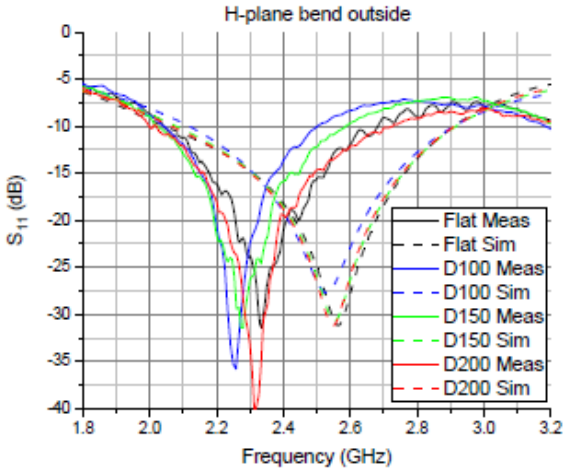

Radiation patterns of flat antennas

The maximum realized antenna gain and radiation pattern have been measured in horizontal and vertical planes for the patch and bow-tie antennas. Figures 15 and 16 illustrate the maximum realized gain of the patch antenna. The simulation results are lower than the measured one by 0.8-0.5dBi. However, there are no such discrepancies in the bow-tie results. The dimensional variations or effect of connectors have been investigated, and the only reasonable explanation could be that the additional fringing fields (π-shaped edges) can have an enhanced effect in the resonance antenna types (Figure 17).

Figure 15. Maximum realized gain vs. frequency for the patch antenna with Sylgard 170 as dielectric and various conducting polymers.

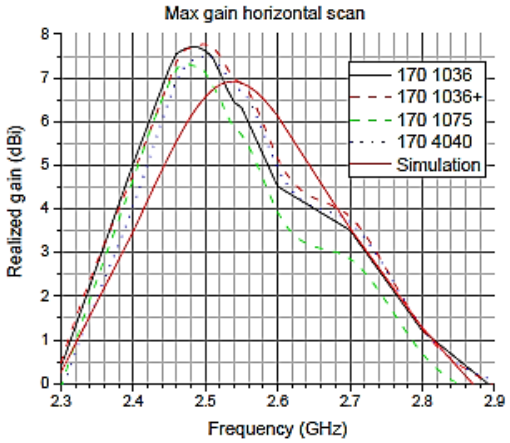

Figure 16. Maximum realized gain vs. frequency for the patch antenna with modified EG3896 as dielectric and various conducting polymers.

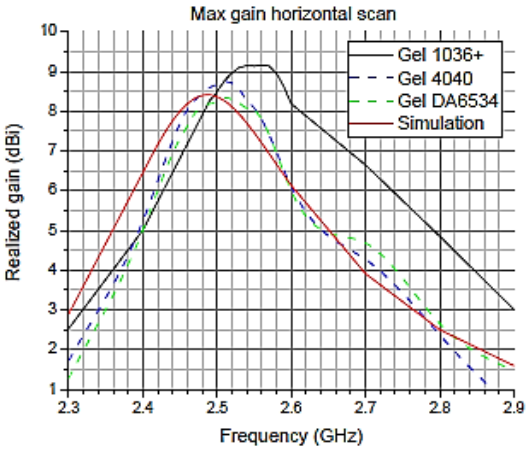

Figure 17. Maximum realized gain vs. angle for the patch antenna with modified EG3896 as dielectric and various conducting polymers at 2.5 GHz.

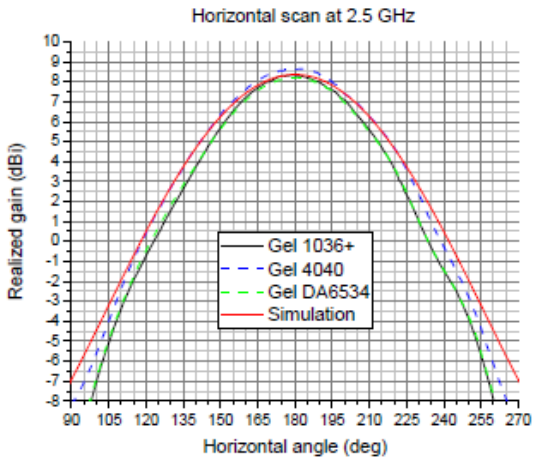

The maximum realized gains for the patch antennas are7.76 dBi and 9.16 dBi with Sylgard 170 and modified EG3896.The conductivity variations give 0.3-0.5 dBi degradation when the conductivity is above 106 S/m. While the reduction of conductivity below 106 S/m can have a significant reduction in the realized gain, as it has been shown in Figure 18 for the bowtie antenna.

Figure 18. Maximum realized gain vs. frequency for the bow-tie antenna with Sylgard 170 as dielectric and various conducting polymers.

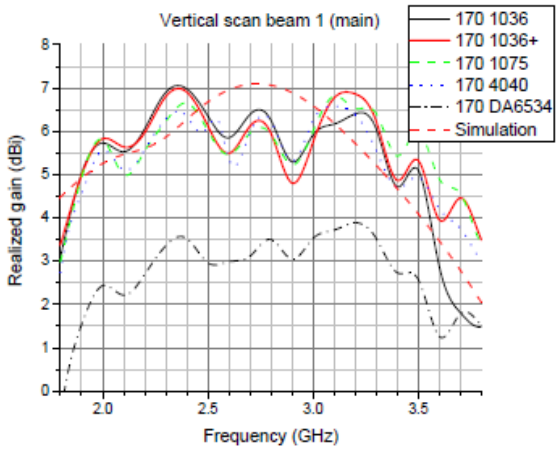

The patch antennas with Sylgard 170 have the 3 dB bandwidth in horizontal and vertical planes around 74 degrees in measured and 78 degrees in simulated data with no effects from conductivity (Figure 19). Although, modified EG3896 has some variations from 60 deg with CI-1036+ to 68 deg with CI-4040 in the horizontal plane. While the vertical plane scan shows 79 deg with CI-1036+ and 70 deg with CI-4040. The level of cross-polarization varies from -35 dBi to -17 dBi with the conductivity and dielectric loss. The measured data shows that the level of cross-polarization is directly proportional to losses. This level stays below -20 dB for all cases.

Figure 19. Maximum realized gain vs. angle for the bow-tie antenna with Sylgard 170 as dielectric and various conducting polymers at 2.5 GHz. 275 deg is the main lobe direction.

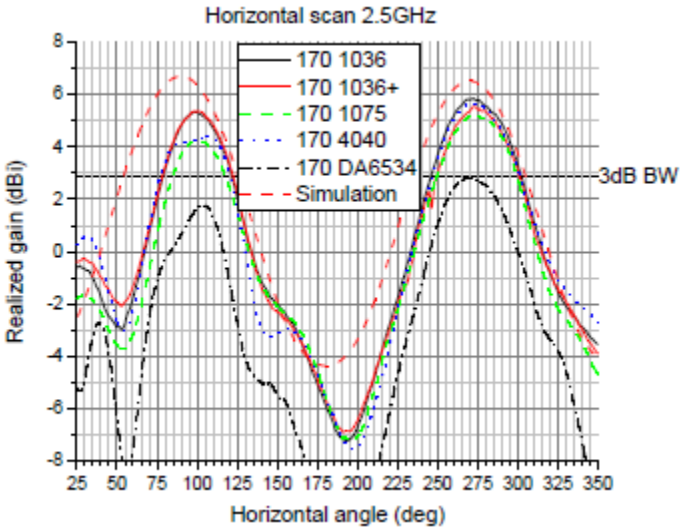

The maximum realized gains for the bow-tie antennas are 7.1 dBi and 7.9 dBi with Sylgard 170 and modified EG3896. Figure 20 shows the spike at 3.1 GHz; this is cumulative radiation from the antenna and the feeding network. The feeding network has 50 mm length, which is exactly half- wavelength at 3.1 GHz.

The bow-tie antennas with Sylgard 170 have the 3 dB bandwidth in the vertical plane around 74 degrees and 56 degrees in the horizontal plane with no variations from conductivity. However, modified EG3896 shows a similar behavior as with patch antennas case. Cl-1036+ has 72 deg in the vertical plane and 49 deg in the horizontal plane, while Cl- 4040 shows 60 deg and 55 deg in the vertical and horizontal plane (Figure 21). The level of cross-polarization stays below -16 dB for Sylgard and -25 dB for modified EG3896 and degrades with a reduction of conductivity.

Figure 20. Maximum realized gain vs. frequency for the bow-tie antenna with modified EG3896 as dielectric and various conducting polymers.

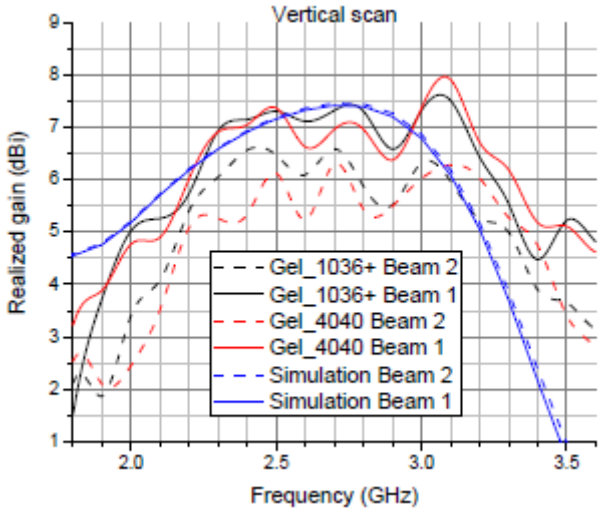

Figure 21. Maximum realized gain vs. angle for the bow-tie antenna with modified EG3896 as dielectric and various conducting polymers at 2.5 GHz.

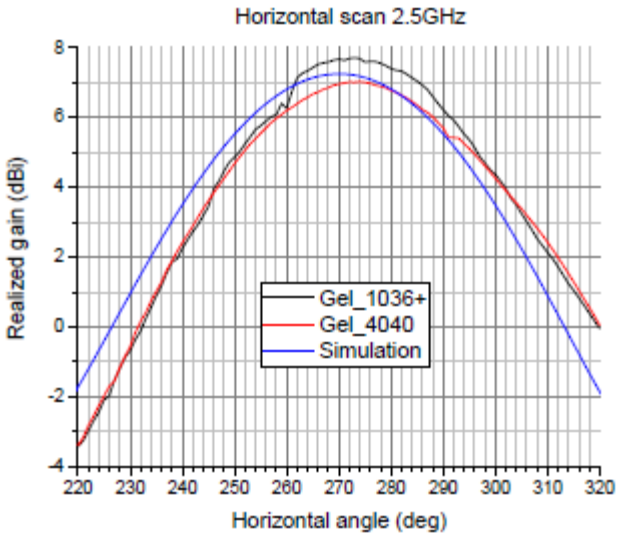

Radiation patterns of bent antennas

The effect of bending on the radiation patterns have been investigated for both types of antennas. The E-plane bend inside on Figure 22 and exhibit significant improvements in the realized gain, while other types of deformations show only reductions in the gain.

Figure 22. Measured and simulated realized gain vs. frequency for the bent in E- plane inside patch antenna with modified EG3896.

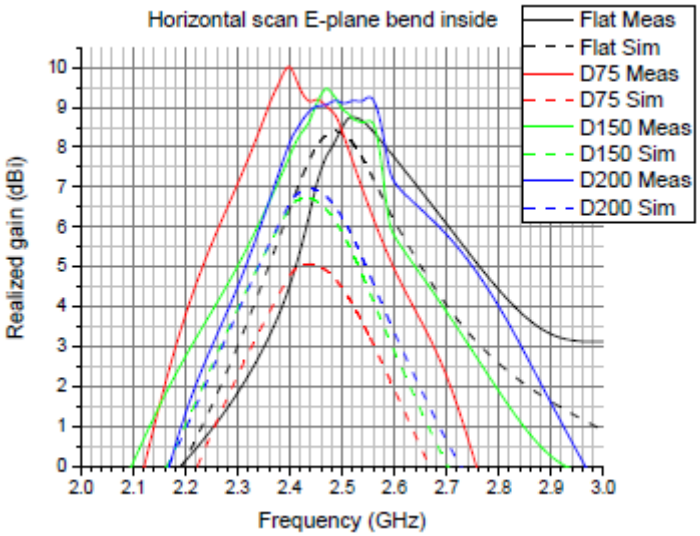

The reflection coefficient shifts left with bending with minor improvements in matching conditions, which is no enough to explain rising in the gain from 8.6 dBi to 10.1 dBi for patch antenna. The bow-tie antenna shows improvements from 7.34 dBi to 8.38 dBi at 2.5 GHz and at the maximum peaks from 7.9 dBi to 11.3 dBi. Puzzlingly that CST simulation results fail to predict any gain effects for the patch antenna and manages to show some improvements for the bow-tie. Although generally, the simulations results are very close to measured, there are discrepancies at 3.1 GHz due to additional contribution from the feeding network radiation, and it has not been reflected in the simulation results. As it has been seen in the patch antenna that simulations results are underestimated for the antenna gain due to probable excessive fringing fields as shown in Figure 23.

Figure 23. Measured and simulated realized gain vs. frequency for the bent in E-plane outside patch antenna with modified EG3896.

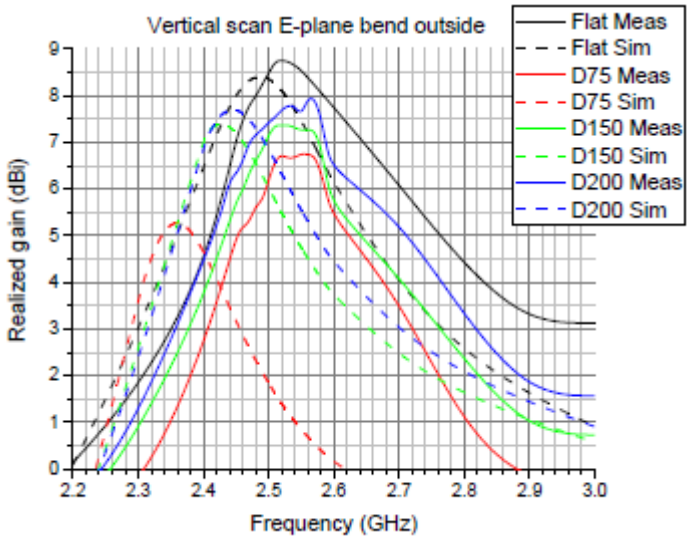

It seems that the general trend of the gain improvements with E-plane bend inside might come from the focusing effect. The 3 dB bandwidth of the beam in Figures 24 and 25 changes with the curvature in the vertical plane, i.e., 79 degrees is in the flat condition, 66 degrees with D200, 59 degrees with D150, and 49 degrees with D75. The 3 dB bandwidth in the horizontal plane remains around 60 degrees with all curvatures in measured data at 2.5 GHz for the patch antenna.

Figure 24. Measured and simulated realized gain vs. angle for the bent in E-plane outside patch antenna with modified EG3896 at 2.5 GHz.

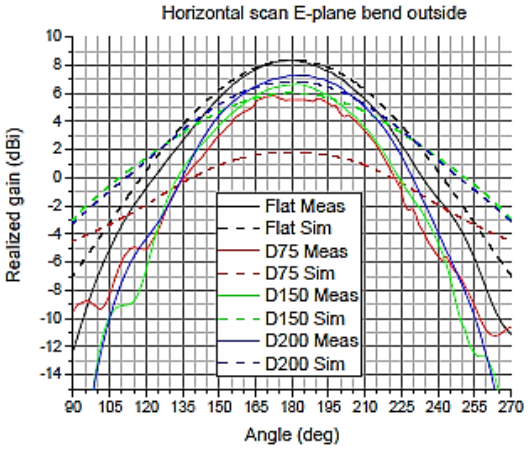

Figure 25. Measured and simulated realized gain vs. frequency for the bent in E-plane inside bow-tie antenna with modified EG3896.

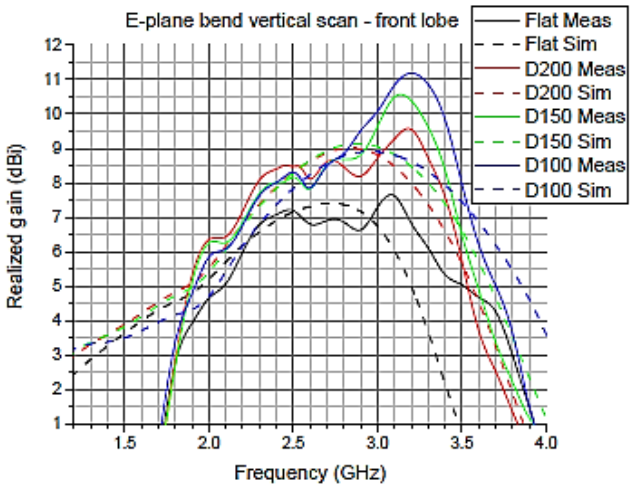

The bow-tie antenna does not exhibit such big changes at 2.5 GHz. Even though there is 1.3 dBi improvement with D200 curvature, the 3 dB bandwidth narrows down just by 5 degrees in the horizontal and 2 degrees in the vertical plane. The further bending has a negative effect, and the 3 dB bandwidth widens. However, the nulls become closer proportionally to the curvature (Figure 26). The most drastic effect is being seen at 3.1-3.2 GHz. The 3 dB bandwidth reduces from 92 degrees in the flat to 47 degrees at D100 with a similar reduction of the angle between nulls.

Figure 26. Measured and simulated realized gain vs. frequency for the bent in H plane inside bow-tie antenna with modified EG3896.

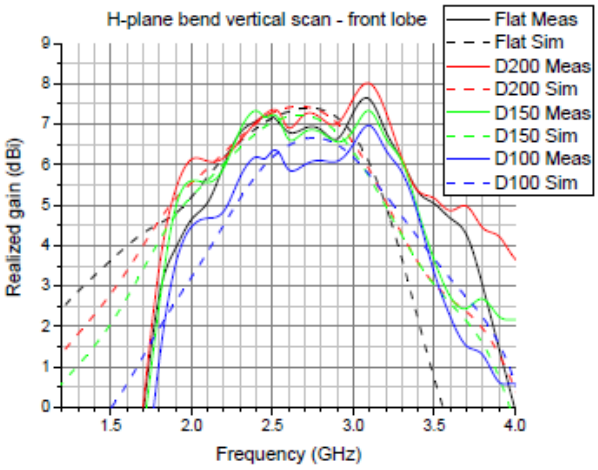

The back lobe of the bow-tie antenna exhibits bending outside (Figure 27) illustrates that the beam is splitting at certain curvatures. This can be explained that the elements of the antenna become orthogonal, and produced EM fields no longer complement each other. The 3 dB bandwidth is rapidly increasing, the realized gain is decreasing, and the angle between nulls is rising. The H-plane and E-plane bend outside for the investigated antennas cause only degradations. Although, certain curvatures in H-plane with bending inside can have slight improvement effects as for the patch and for the bow-tie antennas. The patch antenna gains an additional 0.5 dB at the D200 and then reduced by 3 dB at D75, without any frequency shifts. The bow-tie antenna gains up to 1 dB at D200, then up to 0.6 dB at D150, and then the realized gain drops by 1 dB at D100 (compare to the flat condition).

It is necessary to mention that all antennas have been aligned to the maximum gain at 2.5 GHz, but the main lobe direction is drifting with frequencies. That's why measured graphs have wavy shapes. For the same reason, the measured gains and bandwidth might be not exactly as they are, but fairly close.

Figure 27. Measured and simulated realized gain vs. angle for the bent in E-plane inside bow-tie antenna with modified EG3896 at 2.5 GHz.

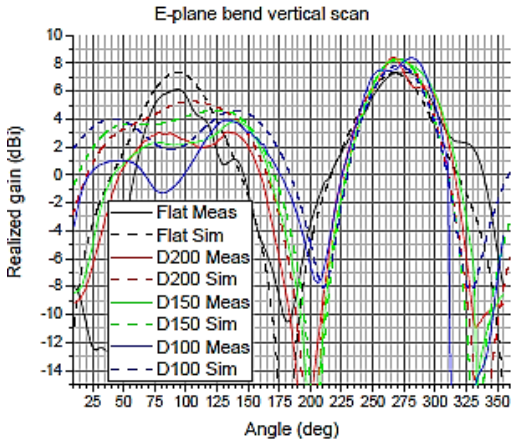

Summary of materials effects on the antenna performance

It is undeniable that any loss has a negative effect, and it is desirable to have as better conductivity as possible and lower dielectric loss. Unfortunately, we must sacrifice one or another parameter in order to achieve flexibility. Figures 28 and 29 illustrate the measured and simulated data of conductivity and dielectric loss effects for the bow-tie and patch antennas. The data is fair for these types of antennas and might be different for others. The two dots in Figure 28 are CI-1075 polymers (≈$4*10^6$ S/m), and they are out of the trends. This particular polymer in our batch has some problems in consistency. The polymer has flecks, and measured conductivity varies from sample to sample. These two dots can be excluded from further discussion.

Figure 28. Measured and simulated relations between the realized antennas gain and conductivity at 2.5 GHz.

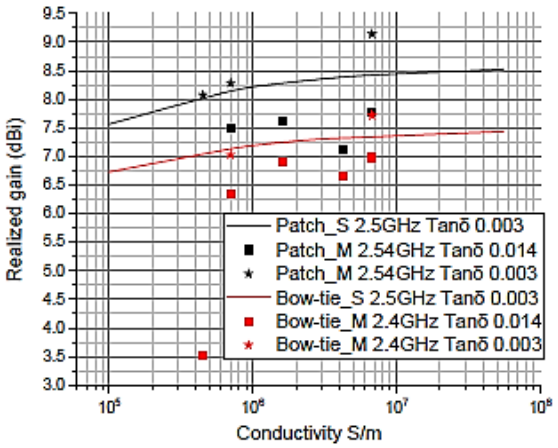

The dielectric loss has a greater effect on the patch antenna rather than on the bow-tie. The slope of the curves in Figure 29 indicates that dielectric loss below 0.01 is not desirable, and other types of antennas can be considered for better performance, e.g., the bow-tie or might be even simple dipoles if there is no choice in the dielectric materials. The dielectric loss can be greatly reduced by proper material selection and compounding. Although, there is a plateau where further dialectic loss reduction does not give significant benefits at a certain operational frequency. The measured data follows the simulated trends but has some discrepancies due to various reasons, e.g., variations in the surface roughness, consistency, measured errors, fielding fields, etc.

The ohmic loss has similar trends as for the dielectric loss, and it can be noticed that the slope increases at the conductivities below 10^6 S/m. However, the measured trends indicate that the bow-tie antennas are more sensitive for low conductivity, and the measured slope is way greater than for the patch antennas. The further improvements of the conducting polymers are rather challenging, inevitably reduces the ability to stretch, and can benefit for a small margin. Although, it is fair for the antennas themselves with a relatively simple feeding network, and it must be reconsidered for the complex feeding networks as in antenna arrays. The experimental results show that the conductivity around 10^6 S/m is a sweet spot since it allows to engineer the mechanical properties and find the optimum trade-off between conductivity and flexibility with minimum efforts. The further material improvements might be directed towards the reduction in the dielectric losses. It will allow us to raise the operational frequencies for the flexible polymer-based microwave electronics.

Figure 29. Measured and simulated relations between the realized antennas gain and dielectric loss at 2.5 GHz.

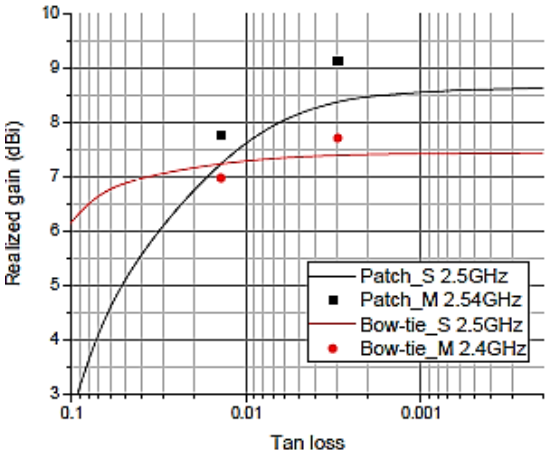

Comparison with other flexible antennas

Some antennas exhibit semi-rigid properties due to very thin structure, even though they have been produced from rigid substrates, e.g., RO4003 or Duroid 5880. The same can be extended to the Kapton (polyimide), PET, PEN, LCP, Teflon (PTFE), and other plastic substrates. These type of plastics does not exhibit elastomer's properties and can be used for flexible microwave electronics within certain thickness constrains. The usage of metals and rigid inks for the conducting materials has its own limits too, due to their extremely small elongations (1% or less) (Table 4).

Table 4. summarizes antennas' performance of flexible antennas.

Performance of flexible antennas in the flat condition				
Antenna type, ref	**Dielectric, thickness**	**Conductor, thickness**	**Operational frequency**	**Antenna gain**
Patch, this work	Mod PDMS,3 mm	Polymer, 70-100 um	2.45-2.58	7-9.16 dB
Patch, [14]	PDMS (Sylgard 184), 3.18 mm	Fabric NCS95R-CR, 130 um	2.28-2.32	2.9-3.3 dBi
Patch, [15]	Unknown rubber, 1.4 mm	Polymer PE873,30 um	2.35-2.45	0.9 dB
Patch, [16]	NinjaFlex, 1.2 mm	Polymer PE873,30 um	1.94-2.93	-7.2 dB
Patch, [17]	PDMS,1.6 mm	VeilShield mesh, 57 um	2.35-2.55	1.8 dBi
Bow-tie,this work	Mod PDMS,3 mm	Polymer,70-100 um	2-2.8	5-7.9 dBi
Bow-tie, [18]	PET, 135 um	Silver ink, 3.7 um	2.1-4.35	4-6.3 dB Simulation
Bow-tie, [19]	Duroid 5880,787 um	Copper,35 um	0.81-1.87	3.8-4.78 dBi
Bow-tie, [20]	RO4003C,200 um	Copper,35 um	2.2-4	2.2-6.3
Bow-tie,[21]	Leather,900 um	Ag-ink,unknown	1.48-1.7	-2.5 dBi

Several patch antennas were produced with PE873 polymer but do not exhibit good performance (0.9 dB, -7.2 dB). This happens due to the paintbrush production process. The pain brush technique does not give acceptable precision in xy-plane but also lacking any control on the final layer thicknesses. The produced layers can have variations from few microns to several dozen microns, which will create a random pattern with high resistant areas, areas with excessive radiations, and increase the surface roughness. Additionally, the polymer integration must be done to avoid layer separations and misplacements of the conducting layers. Apparently, the surface roughness has had a great effect on the performance of bow-tie antenna on the leather substrate, even with relatively high conductivity of silver ink around 8-9*10^5 S/m and dielectric loss around 0.07. The moderate performance of antennas on the classical Roger and Duroid substrates with copper cladding might be due to design specifics.

CONCLUSION

This work demonstrates that proper material selection, material engineering, and production process of polymer-based flexible microwave electronics can achieve competitive performance compare to rigid PCB technology. Classical designs of the patch and bow-tie antennas have been realized with various polymers to investigate the effects of the dielectric loss and conductivity on the antennas' performance in S-band in order to find acceptable limits for further flexibility improvements.

The proposed recipes for low-loss, low-Dk dielectric materials, and chemical integration between conducting polymers and PDMS have been presented and tried on several microwave devices. The current molding process allows us to step out from 2D PCB designs and build 3D structures or hybrid PCB-3D components with a certain

freedom in material properties. Additionally, the new material exhibits unique mechanical properties, i.e., low density, temperature insulation, vibration and acoustic dumping effects, low humidity absorption, and so on, which extends the material application to other fields.

The antenna's structures have non-classical features like π- shaped edges, which lead to additional fringing fields. It seems that the fringing fields have an effect on the resonance type of antennas like the patch antenna; if so, then it is possible to have enhanced antenna gain by intentional shaping of conductors. However, it is still a subject of investigation whether the fringing fields are the reason and what simulation techniques can predict accurately such effects.

The bending effects have been investigated too, and it has been demonstrated that e-plane bend inside can have the focusing effect and boost the antenna gain. This can be exploited by producing pre-shaped structures of classical antennas either by current production technique or 3D printing, which might benefit not only stand-alone antennas but arrays too.

ACKNOWLEDGMENT

The authors gratefully acknowledge support from Dow Corning chemical department of Singapore and 3M, Nouryon companies for provided samples. As well as to the Siberian Federal University for financial support within the framework of the FSRZ-2023-0008 program.

REFERENCES

1. Veeraselvam, et al. Polarization diversity enabled flexible directional UWB monopole antenna for WBAN communications. Int. J. RF Microw. Comput. Eng. 2020;30:e2231.
2. H. Lee, et al. Flexible spiral antenna with microstrip tapered infinite balun for wearable applications. IEEE Antennas Propag. Soc. AP-S Int. Symp.2012.
3. Q. H. Abbasi, et al. Ultrawideband band-notched flexible antenna for wearable applications. IEEE Antennas Wirel. Propag. Lett. 2013;12:1606-1609.
4. F. Tariq, et al. A flexible antenna on cost-effective PEN substrate for sub-6 GHz 5G wireless transceivers. Int. Conf. Front. Inf. Technol. 2019;89-94.
5. Y. Zhou, et al. Mechanical and high-frequency electrical study of printed, flexible antenna under deformation. IEEE Trans. Components, Packag. Manuf. Technol. 2020;10:1088-1100.
6. K. K. Naik, et al. Design of flexible parasitic element patch antenna for biomedical application. Prog. Electromagn. Res. M. 2020;94:143-153.
7. M. Rizwan, et al. Flexible and stretchable 3D printed passive UHF RFID tag. Electron. Lett. 2017;53:1054-1056.
8. S. M. Alqadami, et al. Assessment of PDMS technology in a MIMO antenna array. IEEE Antennas Wirel. Propag. Lett. 2016;15:1939-1942.
9. Cherukhin, et al. Performance improvements in flexible polymer-based microwave devices. Asia-Pacific Microw. Conf. Proceedings, APMC. 2019;619–621.
10. Cherukhin, et al. Investigation of material properties for polymer-based microwave devices. J. Phys. Conf. Ser. 2019;1399:4.
11. Cherukhin, et al. Fully flexible polymer- based microwave devices: materials, fabrication technique, and application to transmission lines. EEE Trans. Antennas Propag. 2021;69:8763-8777.
12. Larmagnac, et al. Stretchable electronics based on Ag-PDMS composites. Sci. Rep. 2014;4:1–7.

13. M. Park, et al. Design of conductive composite elastomers for stretchable electronics. Nano Today. 2014;9:244–260.
14. R. B. V. B. Simorangkir, et al. A method to realize robust flexible electronically tunable antennas using polymer-embedded conductive fabric. IEEE Trans. Antennas Propag. 2018;66:50–58.
15. Y. Song, et al. Polymer-based 2.4 GHz patch antenna. Int. Work. Antenna Technol. 2020;7–10.
16. M. Rizwan, et al. Flexible and stretchable brush-painted wearable antenna on a three-dimensional (3-D) printed substrate. IEEE Antennas Wirel. Propag. Lett. 2017;16:3108–3112.
17. S. M. Sayem, et al. Robustness analysis of the polymer-conductive-mesh composite for the realization of transparent and flexible wearable antennas. 2020 14th Eur. Conf. Antennas Propagation. 2020;1–4.
18. M. A. Riheen, et al. CPW fed wideband bowtie slot antenna on pet substrate. Prog. Electromagn. Res. C. 2020;101:147–158.
19. R. Sahoo et al. Bow-tie-shaped wideband conformal antenna with wide-slot for GPS application. Turkish J. Electr. Eng. Comput. Sci. 2019;27:80–93.
20. M. O. Sallam, et al. Wideband CPW-fed flexible bow-tie slot antenna for WLAN/WiMax systems. IEEE Trans. Antennas Propag. 2017;65:4274–4277.
21. M. F. Farooqui et al. Dual band inkjet printed bow-tie slot antenna on leather. Eur. Conf. Antennas Propagation, EuCAP. 2013;3287–3290.